A novel analytical strategy for rapid detection of antibiotic dregs adulteration in feed protein materials by headspace gas chromatography–ion mobility spectrometry

Shouxue Li[1], Yuchao Feng[2], Yushu Zhang[3], Xia Fan[2]*

[1]Jiangsu Vocational College of Agricultural and Forestry, Jurong, Jiangsu, P.R. China; [2]Institute of Quality Standards and Testing Technology for Agro-Products of Chinese Academy of Agricultural Sciences, Beijing, P.R. China; [3]College of Food, Heilongjiang Bayi Agricultural University, Daqing, P.R. China

***Corresponding Author:** Xia Fan, Institute of Quality Standard and Testing Technology for Agro-Products, Chinese Academy of Agricultural Sciences, Beijing, China. Email: fanxia@caas.cn

Academic Editor: Aziz A. Fallah, PhD. Department of Food Hygiene and Quality Control, Faculty of Veterinary Medicine, Shahrekord University, Shahrekord, Iran

Received: 8 April 2024; Accepted: 17 December 2024; Published: 16 January 2025

ORIGINAL ARTICLE

Abstract

The recognized shortage of feed protein materials (FPM), together with their high prices, has almost inevitably led to economically motivated adulteration. In this study, a rapid and accurate headspace gas chromatography–ion mobility spectrometry (HS-GC-IMS) method was applied to detect soybean meal (SM) and cottonseed meal (CM) adulteration with oxytetracycline dregs (OD). A total of 98 volatile compounds were detected in the 14 samples (5 SM, 5 CM, and 4 OD). FPMs and adulterated FPMs in different proportions (0.1, 0.5, 1, and 5%, w/w) were classified based on their volatile compounds using principal component analysis (PCA) and orthogonal partial least squares discriminant analysis (OPLS-DA). The OPLS-DA model could identify SM-adulterated samples with an OD content of 0.5–5% and CM-adulterated samples with an OD content of 1–5%. More importantly, 18 volatile compounds (ether and heterocycle [1 each], acids and terpenes [2 each], and ketones, alcohols, aldehydes, and esters [3 each]) were proposed as volatile markers for OD authentication from FPMs. These results confirmed the potential of HS-GC-IMS to evaluate volatiles in FPMs and are meaningful for FPMs quality. The environmental factors and sample differences will be investigated in future studies to improve the robustness and reliability of HS-GC-IMS.

Keywords: feed safety; headspace-gas chromatography-ion mobility spectrometry; multivariate statistical analysis; volatile organic compounds

Introduction

In the context of food and feed safety in today's world, it has become an industrial trend to reduce the amount of soybean meal and replace it with unconventional feed protein (Harris *et al*., 2018; Kim *et al*., 2019; Mottet *et al*., 2017). However, with the development and utilization of different types of feed protein materials, several risky substances have emerged, resulting in increasingly prominent feed and animal product safety issues.

Oxytetracyclinedregs (OD)are the most productive type of antibiotic dregs and are mainly composed of mycelia, remaining medium, trace antibiotics, and unknown fermentation intermediates (Guo *et al*., 2012). OD contains high nutritional content, similar to the conventional chemical composition of feed protein materials (Mohring *et al*., 2009). However, the residual antibiotics and unknown secondary metabolites in them have brought great risks to the aquaculture industry (Li *et al*., 2016). Owing to the global shortage of feed protein materials,

 ISSN 1757-837X online, DOI 10.15586/qas.v17i1.1517

the market price continues to rise. In contrast, the cost of antibiotic dregs is extremely low. Driven by economic interests, some unscrupulous farmers add antibiotic dregs to feed protein materials to increase their profit. Therefore, it is imperative to effectively monitor the risks of substances in feed protein materials.

A literature search showed that the main method used to determine whether antibiotic dregs were added to the feed or not was to detect antibiotic residues. Analytical techniques based on liquid chromatography–tandem mass spectrometry, gas chromatography–mass spectrometry, liquid chromatography–time-of-flight mass spectrometry, and other large instruments are the most widely used for detecting antibiotic residues (Lin *et al*., 2018). These methods include complicated and time-consuming sample preparations, the equipment is inconvenient and expensive, and the procedures have several limitations in identifying non-target risk substances (Kranenburg *et al*., 2020). The feasibility of attenuated total reflectance–infrared and microscopic infrared (IR) imaging for the rapid identification of OD in feed protein materials was previously investigated (Li *et al*., 2021). The results showed that microscopic IR imaging combined with chemometrics could detect 1% OD (w/w) in soybean and cottonseed meal. However, these spectral methods require a large number of samples and complicated statistical procedures for constructing adulteration models, which might restrict their application in quality inspection agencies (Rodríguez *et al*., 2019).

Each agri-food product has a distinct odor composed of hundreds of volatile organic compounds (VOCs), and odor change is one of the most sensitive indicators of agri-food quality (Gu *et al*., 2021). Consequently, VOCs emitted from agri-food can be used to define sample data, which can accurately depict the relationship between changes in volatile components and the quality of agri-food products (Hernández-Mesa*et al*., 2019). Headspace gas chromatography–ion mobility spectrometry (HS-GC-IMS) has emerged as a promising technology for the accurate characterization and detection of VOCs in agri-food products (Wang *et al*., 2020; Zhang *et al*., 2020). The separation capacity for resolving complex matrices is enhanced when GC and IMS are combined. When IMS was used with GC pre-separation, the detection accuracy was enhanced compared to that of IMS alone. This technology operates at atmospheric pressure and combines the advantages of portability, rapid analysis without sample pretreatment, and ease of operation for adulteration detection. Based on the differentiation of volatile profiles, especially characteristic markers, between adulterants and pure samples, HS-GC-IMS has been used to detect adulteration in quinoa flour (Yang *et al*., 2022), bovine milk (Tian *et al*., 2023), honey (Arroyo-Manzanares *et al*., 2019), and oil (Dou *et al*., 2022). Till date, no studies have been conducted to develop methods using HS-GC-IMS technique for the rapid detection of adulteration in feed protein materials.

Hence, the main objective of this study was to investigate the feasibility of using HS-GC-IMS combined with chemometrics for the rapid and accurate authentication of oxytetracycline dregs in feed protein materials, such as soybean meal (SM) and cottonseed meal (CM). The specific aims were to 1) characterize the VOCs in SM, CM, OD, and adulterant samples; 2) visually explore the volatile profile differences of pure and adulterated feed protein materials by fingerprint analysis; and 3) build discrimination models for feed protein materials and adulterants using principal component analysis (PCA) and orthogonal partial least squares discriminant analysis (OPLS-DA), and then propose key volatile markers.

Materials and Methods

Samples

In this study, 14 samples were obtained commercially, based on the principle of wide representativeness. Five SM samples (SM01–SM05) and five CM samples (CM01–CM05) were obtained from manufacturers in Shandong, Jiangsu, and Sichuan provinces. Four OD samples (OD01 to OD04) were obtained from manufacturers in the Shandong and Hebei provinces. The samples were stored at −20°C before use. The quality and authenticity of the samples were guaranteed by the manufacturers.

The SM adulterants were prepared by mixing OD (01–04) and SM (01–04) at ratios of 0.1:99.9, 0.5:99.5, 1:99, and 5:95 (w/w). The CM adulterants were obtained by mixing OD (01–04) and CM (01–04) at the same ratios.

HS-GC-IMS

Volatiles of the samples were analyzed using an IMS instrument (FlavourSpec, Gesellschaft für analytische Sensorsysteme mbH, Dortmund, Germany) with an internally installed Agilent 990 gas chromatograph (Agilent Technologies, Palo Alto, CA, USA), referring to the methods of previous reports with some modifications (Yang *et al*., 2021; Zhang *et al*., 2020).

Samples (2.0 g) were weighed and transferred into a 20 mL headspace glass sampling vial. They were then incubated at 80℃ for 20 min in an autosampler. After incubation, 500μL of headspace gas was injected into the injector (85℃, splitless mode). The injected samples were driven into an FS-SE-54-CB-1 capillary column (15 m × 0.53 mm, Agilent Technologies) under 60℃ isothermal

conditions using nitrogen (99.999% purity) as the carrier gas. The carrier gas was passed through the HS-GC-IMS injector, and the sample was transferred to the GC column as follows: 2 mL/min for 2 min, 10 mL/min for 8 min, 100 mL/min for 10 min, and 150 mL/min for 10 min until the flow stopped. After GC separation, the analytes were ionized in the IMS ionization chamber in positive ion mode by a β-radiation-^{3}H ionization source with 300 MBq activity. The ions were driven to the drift tube at 45 ℃ on a constant tube linear voltage (400 V/cm) with a nitrogen flow of 150 mL/min as the drift gas. The drifted ions were captured in 30 ms.

The RI of each compound was calculated using n-ketones C4~C9. All VOCs were qualitatively analyzed by comparing their respective RI and drift time to those of standards in the IMS database and the built-in NIST database. Spectrograms were analyzed using Laboratory Analytical Viewer software (Gesellschaft für analytische Sensorsysteme mbH, Dortmund, Germany). Visual representations of two- and three-dimensional top views were recorded using the Reporter plug-in, and fingerprint comparison was intuitively constructed using a Gallery Plot plug-in.

Data analysis

Qualitative analysis of the volatile components was performed based on the built-in database of the GC × IMS library. Principal component analysis (PCA) and orthogonal partial least squares discriminant analysis (OPLS-DA) were performed using the SIMCA software (version 14.1 Umetrics, Umea, Sweden). R^2X and R^2Y explain the variations in variables X and Y, respectively, whereas Q^2 (cum) indicates the predictive ability of the developed discrimination method. All of them range between 0 and 1, and the values closer to 1 indicated a better fit of the model. Concerning the Q^2 parameter, a significant threshold of 0.5 is generally acceptable, for that reason the model achieves a good predictive ability. The variable importance of projection (VIP) was the vector to summarize the total importance of the variable in explaining the model. A VIP value greater than 1 is considered a critical variable in a given model (Song *et al.*, 2020). Validation of the models against an independent test set was impractical owing to the limited number of samples involved in this study; as such, only a cross-validation (CV) approach was applied to assess the model performance.

Results and Discussion

HS-GC-IMS topographic plots

Figure 1 shows a two-dimensional (2D) array full-size top view of representative samples consisting of the ion drift time (X-axis) and retention time of gas chromatographic peaks (Y-axis). Each point on the spectrum represents a volatile component, and its color indicates the signal intensity. Most signals for SM and CM samples were detected with drift times from 1.0 to 1.75 and retention times from 100 to 530 s. The topographic plot of SM was similar to that of CM although they showed different intensities for several signals with the same drift and

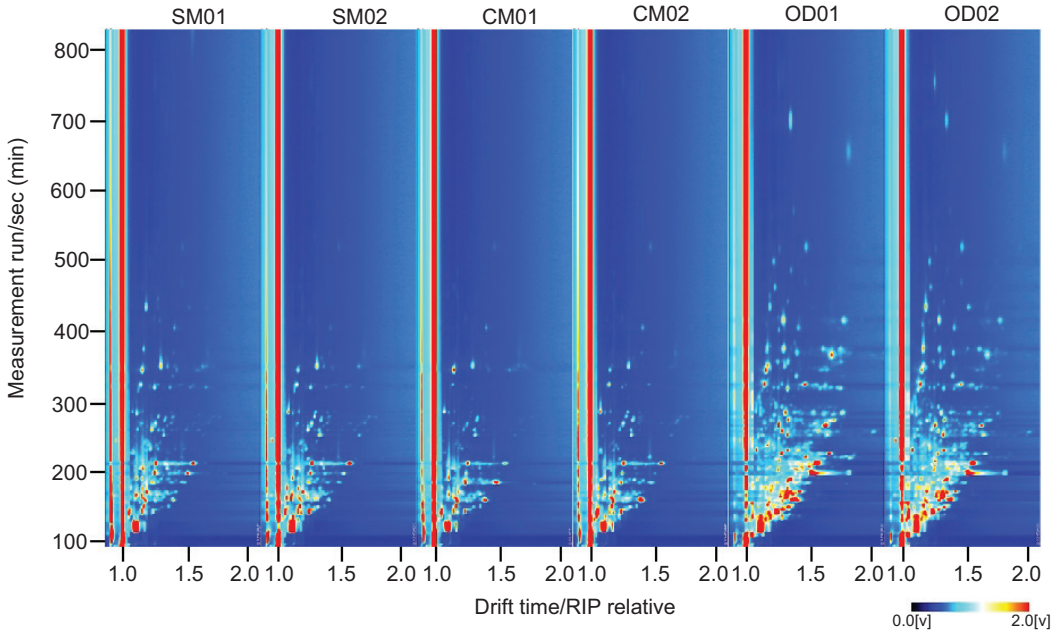

Figure 1. 2D topographic plots of SM, CM and OD.

retention times. The main signals for OD samples were detected with drift times from 1.0 to 2.18 and retention times from 100 to 770 s. SM and CM exhibited different topographic plots from that of OD, especially during the retention time from 360 to 770 s. The differences in the topographic plots among the different types of pure samples indicated potential variance in their volatile profiles.

A different comparison model of the internal software was applied to distinguish the volatile compound characteristics between the FPMs and OD samples. The topographic plot of SM03 was selected as a reference and deduced from the SM and OD sample plots, as shown in Figure 2(A). The topographic plot of the SM samples was similar to that of the reference, as most of its background after deduction was nearly white, although there was some blue background, especially SM1. There was a large red background in the OD samples, which indicated that the concentrations of many volatile compounds in the OD samples were slightly higher than those in the reference. As shown in Figure 2(B), when sample CM03 was used as the reference, CM01 showed a relatively white background, whereas CM02, 04, and 05 exhibited obvious red signals. The OD samples exhibited volatile compounds distinct from those of the CM, as indicated by the visible red signals in their backgrounds. The 2D topographic plot results suggest the potential of HS-GC-IMS to discriminate between pure SM, CM, and OD samples based on their volatile compounds.

Red indicates high intensity, and blue indicates low intensity. The drift time was determined based on normalization of the ion migration time and reactive ion peak (RIP).

Volatile components in pure and adulterated samples

A total of 98 markers were selected after exploration of the 14 pure samples, 88 of which were identified by comparison with authentic reference compounds, 77 were single substances, and 11 were dimers; the results are shown in Table 1. It is worth mentioning that some VOCs with high proton affinity or high concentrations may form dimers or even oligomers. Monomers and dimers of the same substance have similar retention times but exhibit different migration times. Thus, they result in datasets with multiple signal peaks corresponding to one substance.

Among the 88 identifiers, 20 were esters, 17 aldehydes, 17 alcohols, 11 ketones, 10 acids, 7 heterocycles, 4 ethers, and 2 terpenes. In total, 77 volatile compounds, including 67 single compounds and 10 dimers, were identified in the SM samples, while 70 volatile compounds were identified in the CM samples, of which 61 were single substances and 9 were dimers. 88 volatile compounds were identified in the OD samples. The OD samples were solid residues after fermentation for oxytetracycline production, and their composition was more complex.

A gallery plot was generated to determine the differences in volatile compounds in the pure samples. The fingerprints of the pure samples are shown in Figure 3(A), showing 98 compounds. Minor differences between the FPMs and OD samples were found in the concentrations of volatile compounds in the red boxes (Numbers 1–13). Higher concentrations of volatile compounds were found in the OD samples than in the SM and CM samples, as indicated by the green boxes (Numbers 26–83). Notably, the concentrations of volatile compounds (Numbers 84–98) in the OD samples were particularly high, as shown in the yellow box. These volatile compounds might be important for discriminating adulterated samples with OD from SM and CM samples.

The fingerprints of the SM and adulterated samples obtainedare shown in Figure 3(B). The concentrations of(Z)-2-penten1ol (73), butyl propanoate (58), isobutyl butyrate (70), 2-hexanol (80), butyl acetate (66), 2-methylpentanal (47), furfurol (33), and 2-butanone (48) were higher in 1 and 5% adulterated samples than that in SM samples, as shown in the red box. The signal intensity of 2-heptanone (95), citronellol (97), camphene (98), 2,6-dimethylpyrazine (82), and furfurols (76) was higher in only 5% adulterated samples than that in SM samples, as shown in the orange box. However, there was no significant difference between the adulterated and SM (0.1 and 0.5%, respectively) samples. Figure 3(C) shows the fingerprints of the CM and the four adulterated samples. The signal intensities of the substances in the red box, including butanal (61), butyl propanoate (58), 2-hexanol (80), 2-butanone (48), methyl acetate (44), pyrrolidine (39), 3-methylbutyric acid (45), butyl acetate (40), and 3-methyl-3-buten-1-ol (28), were higher in adulterated samples.The signal intensities of most compounds increased as the proportion of OD increased. The concentrations of ethyl acetate(93), 1,8-cineole (75), pentanal (50), 2-heptanone(95), benzaldehyde (57), butyl acetate (66), isobutyl butyrate (70), (Z)-2-penten1ol (73), and 2,6-dimethylpyrazine (82) were higher in only 5% adulterated samples than that in CM samples, as shown in the orange box. The above results indicated the differences in the volatile compounds among the FPMs and adulterated samples with OD. However, it was difficult to identify adulterated samples at low concentrations based only on the differences in volatile compounds.

Multivariate statistical analysis

Principal component analysis is an unsupervised multivariate analysis technique used to reduce the spectral

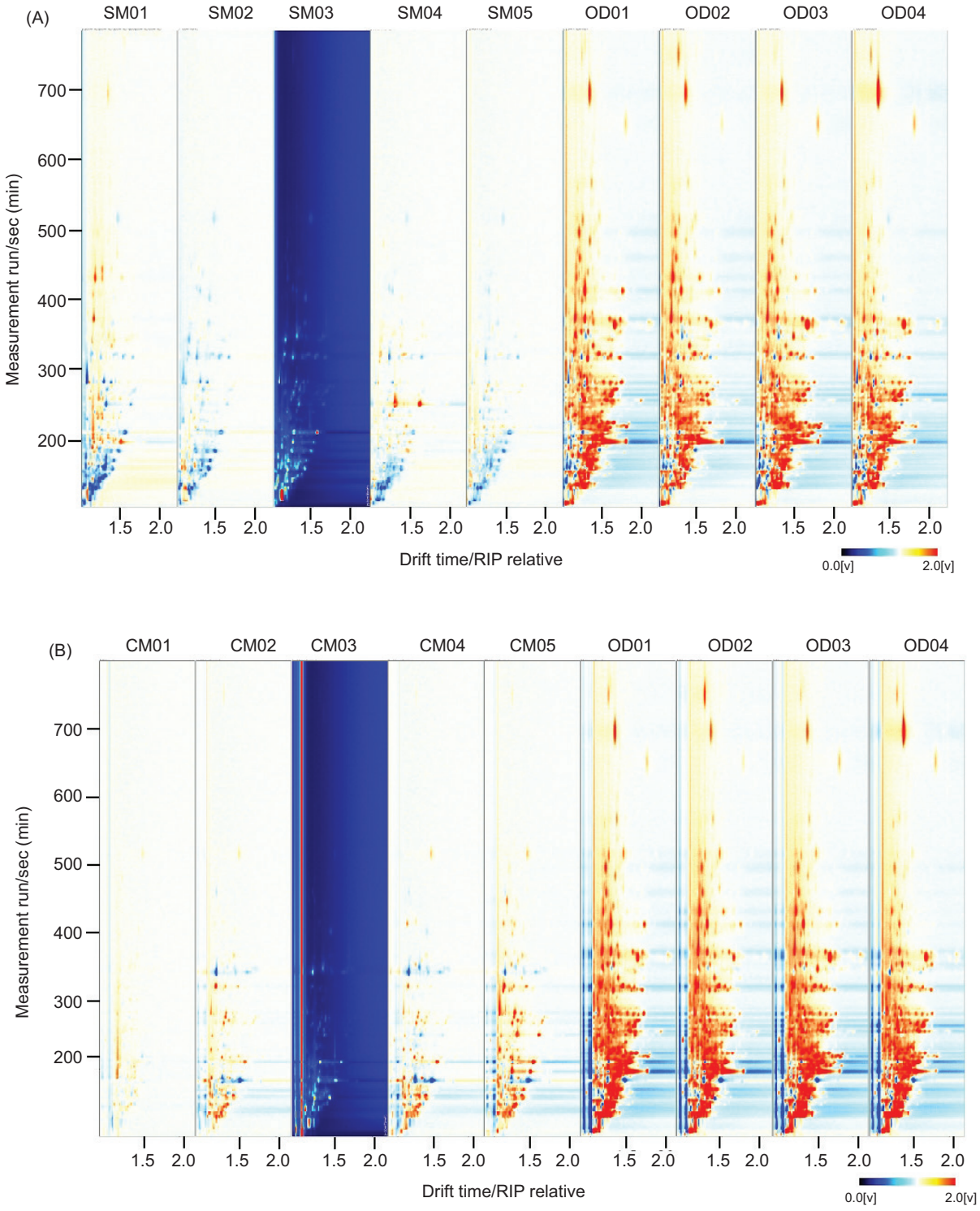

Figure 2. (A) Subtraction topographic plots between SM and OD; (B) Subtraction topographic plots between CM and OD. If the concentrations of VOCs were consistent, the background appeared white; red indicates that the VOC concentration in the samples was higher than that in the reference, while blue indicates a lower concentration.

dimensions in principal components (PC), which captures the maximum data variability and maintains relevant data information. To authenticate adulterants from FPMs, PCA analysis was performed based on the detected signal intensities (a total of 98; Yan *et al*., 2021). The PCA plots are shown in Figure 4. The cumulative variance contribution rates of the first two PCs were 98.76 and 98.96%. From the visualization map, the FPMs and OD samples can be distinguished according to the score values of PC2. However, these models could not

Table 1. The 98 volatile compounds identified from the pure samples.

No.	Compound	CAS#	Formula	MW	RI	RT(S)	DT(a.u.)
1	Hexanal	66-25-1	$C_6H_{12}O$	100.2	783.8	210.425	1.26568
2	Pentanal	110-62-3	$C_5H_{10}O$	86.1	697.9	171.99	1.19724
3	Acetic acid	64-19-7	$C_2H_4O_2$	60.1	595.2	144.038	1.15678
4	Methyl isobutyrate	547-63-7	$C_5H_{10}O_2$	102.1	684.9	166.892	1.1544
5	Ethyl propanoate	105-37-3	$C_5H_{10}O_2$	102.1	705.2	175.284	1.15652
6	Butanol	71-36-3	$C_4H_{10}O$	74.1	651.1	158.272	1.18249
7	3-methylbutan-1-ol	123-51-3	$C_5H_{12}O$	88.1	722.6	183.053	1.49338
8	Hexanal	66-25-1	$C_6H_{12}O$	100.2	790.5	213.95	1.26367
9	2,3-butanedione	431-03-8	$C_4H_6O_2$	86.1	625.2	151.694	1.17392
10	Hexanoic acid	142-62-1	$C_6H_{12}O_2$	116.2	984.2	347.68	1.30303
11	2-Pentanone	107-87-9	$C_5H_{10}O$	86.1	678.6	165.281	1.11001
12	2-Methylpropionic acid	79-31-2	$C_4H_8O_2$	88.1	766.5	202.693	1.16436
13	Hexanal	66-25-1	C6H12O	100.2	784.5	210.766	1.56094
14	Butyl acetate	123-86-4	$C_6H_{12}O_2$	116.2	795.5	216.558	1.23721
15	Unidentified	*	*	0	888.7	265.791	1.54416
16	2-Acetylfuran	1192-62-7	$C_6H_6O_2$	110.1	907.5	280.927	1.1147
17	Pentanoic acid	109-52-4	$C_5H_{10}O_2$	102.1	875.8	258.981	1.23549
18	N-Hexanol(D)	111-27-3	$C_6H_{14}O$	102.2	860.3	250.793	1.32742
19	Thiazole	288-47-1	C_3H_3NS	85.1	744.3	192.75	1.25438
20	Gamma-Butyrolactone	96-48-0	$C_4H_6O_2$	86.1	911.2	284.146	1.08118
21	Butyl propanoate	590-01-2	$C_7H_{14}O_2$	130.2	902.8	276.834	1.28716
22	3-methylbutan-1-ol(D)	123-51-3	$C_5H_{12}O$	88.1	723.3	183.362	1.23951
23	1-Octen-3-ol	3391-86-4	$C_8H_{16}O$	128.2	977.6	341.939	1.15891
24	N-Hexanol	111-27-3	$C_6H_{14}O$	102.2	859.9	250.566	1.64146
25	Acetone	67-64-1	C_3H_6O	58.1	516.1	123.89	1.11537
26	2,3-butanedione	431-03-8	$C_4H_6O_2$	86.1	575.9	139.127	1.18181
27	Hexamethyldisiloxane	107-46-0	$C_6H_{18}OSi_2$	162.4	675.0	164.372	1.32473
28	3-Methyl-3-buten-1-ol	763-32-6	$C_5H_{10}O$	86.1	734.5	188.365	1.15765
29	Benzaldehyde	100-52-7	C_7H_6O	106.1	954.5	321.849	1.1486
30	2-heptanone	110-43-0	$C_7H_{14}O$	114.2	884.9	263.759	1.62804
31	Heptanal	111-71-7	$C_7H_{14}O$	114.2	897.4	272.171	1.33547
32	Butanol(D)	71-36-3	$C_4H_{10}O$	74.1	654.0	159.027	1.38311
33	Furfurol	98-01-1	$C_5H_4O_2$	96.1	818.8	228.847	1.08316
34	2-Propanethiol	75-33-2	C_3H_8S	76.2	542.5	130.599	1.15564
35	Ethyl formate	109-94-4	$C_3H_6O_2$	74.1	619.7	150.271	1.22207
36	Propanoic acid	79-09-4	$C_3H_6O_2$	74.1	668.8	162.78	1.27239
37	Pentanal	110-62-3	$C_5H_{10}O$	86.1	727.4	185.208	1.42292
38	Dipropyl sulfide	111-47-7	$C_6H_{14}S$	118.2	891.9	267.485	1.15181
39	Pyrrolidine	123-75-1	C_4H_9N	71.1	682.5	166.268	1.27199
40	Butyl acetate	123-86-4	$C_6H_{12}O_2$	116.2	823.5	231.348	1.22274
41	Unidentified	*	*	0	872.4	257.161	1.5455
42	6-methyl-5-hepten-2-one	110-93-0	$C_8H_{14}O$	126.2	985.8	349.011	1.17278
43	Gamma-Butyrolactone(D)	96-48-0	$C_4H_6O_2$	86.1	908.7	281.951	1.31131
44	Methyl acetate	79-20-9	$C_3H_6O_2$	74.1	544.7	131.177	1.19342
45	3-methylbutyric acid	503-74-2	$C_5H_{10}O_2$	102.1	833.6	236.693	1.20932
46	2-Furanmethanol, 5-methyl-	3857-25-8	$C_6H_8O_2$	112.1	954.4	321.76	1.55074
47	2-Methylpentanal	123-15-9	$C_6H_{12}O$	100.2	752.0	196.211	1.52202

(*continues*)

Table 1. Continued.

No.	Compound	CAS#	Formula	MW	RI	RT(S)	DT(a.u.)
48	2-butanone	78-93-3	C_4H_8O	72.1	585.3	141.515	1.24354
49	2-Pentanone(D)	107-87-9	$C_5H_{10}O$	86.1	686.2	167.214	1.37305
50	Pentanal(D)	110-62-3	$C_5H_{10}O$	86.1	694.1	170.285	1.42405
51	5-Ethyldihydro-2(3H)-furanone	695-06-7	$C_6H_{10}O_2$	114.1	1048.2	431.638	1.18763
52	2,3,5-trimethylpyrazine	14667-55-1	$C_7H_{10}N_2$	122.2	1007.0	373.292	1.1708
53	Propyl butanoate	105-66-8	$C_7H_{14}O_2$	130.2	905.9	279.567	1.68977
54	Heptanal(D)	111-71-7	$C_7H_{14}O$	114.2	896.9	271.716	1.69447
55	Unidentified	*	*	0	797.4	217.589	1.82532
56	Butanoic acid	107-92-6	$C_4H_8O_2$	88.1	831.2	235.442	1.17241
57	Benzaldehyde(D)	100-52-7	C_7H_6O	106.1	954.4	321.76	1.4665
58	Butyl propanoate	590-01-2	$C_7H_{14}O_2$	130.2	870.0	255.91	1.28447
59	Ethyl hexanoate	123-66-0	$C_8H_{16}O_2$	144.2	991.4	353.914	1.33312
60	Butanoic acid	107-92-6	$C_4H_8O_2$	88.1	763.0	201.101	1.4066
61	Butanal	123-72-8	C_4H_8O	72.1	598.2	144.813	1.28984
62	Unidentified	*	*	0	857.5	249.315	1.13483
63	(Z)-2-Penten1ol	1576-95-0	$C_5H_{10}O$	86.1	759.3	199.448	1.45176
64	2-Ethoxyethanol	110-80-5	$C_4H_{10}O_2$	90.1	730.4	186.546	1.34419
65	Unidentified	*	*	0	754.6	197.348	1.81257
66	Butyl acetate(D)	123-86-4	$C_6H_{12}O_2$	116.2	795.9	216.793	1.61663
67	Pentanoic acid	109-52-4	$C_5H_{10}O_2$	102.1	904.1	277.971	1.22475
68	Sarin	107-44-8	$C_4H_{10}FO_2P$	140.1	800.9	219.409	1.47303
69	Ethyl 3-methylbutanoate	108-64-5	$C_7H_{14}O_2$	130.2	849.6	245.108	1.25897
70	Isobutyl butyrate	539-90-2	$C_8H_{16}O_2$	144.2	948.1	316.238	1.32911
71	(Z)-4-heptenal	6728-31-0	$C_7H_{12}O$	112.2	906.8	280.357	1.6173
72	Unidentified	*	*	0	854.5	247.723	1.09793
73	(Z)-2-Penten1ol	1576-95-0	$C_5H_{10}O$	86.1	770.9	204.626	1.43881
74	Carene	13466-78-9	$C_{10}H_{16}$	136.2	1006.6	372.703	1.29557
75	1,8-Cineole	470-82-6	$C_{10}H_{18}O$	154.3	1035.0	413.014	1.29359
76	Furfurol(D)	98-01-1	$C_5H_4O_2$	96.1	818.8	228.847	1.32943
77	2-methyltetrahydrofuran-3-one	3188-00-9	$C_5H_8O_2$	100.1	818.5	228.733	1.41197
78	2-Methylpropanal	78-84-2	C_4H_8O	72.1	563.9	136.057	1.28581
79	Butanoic acid	107-92-6	$C_4H_8O_2$	88.1	765.2	202.124	1.38714
80	2-Hexanol	626-93-7	$C_6H_{14}O$	102.2	809.7	224.071	1.28112
81	Ethyl acetate	141-78-6	$C_4H_8O_2$	88.1	609.4	147.656	1.33681
82	2,6-dimethylpyrazine	108-50-9	$C_6H_8N_2$	108.1	908.9	282.164	1.53007
83	Unidentified	*	*	0	455.0	108.312	1.1344
84	Unidentified	*	*	0	731.2	186.91	1.0906
85	Amyl acetate	628-63-7	$C_7H_{14}O_2$	130.2	908.3	281.599	1.76224
86	Unidentified	*	*	0	735.9	189.008	1.42292
87	2-Octanone	111-13-7	$C_8H_{16}O$	128.2	1005.4	370.916	1.74588
88	(E, E)-2,4-heptadienal	4313-03-5	$C_7H_{10}O$	110.2	1006.1	371.996	1.60947
89	Benzenemethanol	100-51-6	C_7H_8O	108.1	1034.4	412.189	1.77187
90	Unidentified	*	*	0	983.6	347.145	1.49658
91	Hexanenitrile	628-73-9	$C_6H_{11}N$	97.2	870.1	255.968	1.57301
92	Pentanol	71-41-0	$C_5H_{12}O$	88.1	772.9	205.536	1.49987
93	Ethyl acetate	141-78-6	$C_4H_8O_2$	88.1	572.4	138.218	1.34352

(*continues*)

Table 1. Continued.

No.	Compound	CAS#	Formula	MW	RI	RT(S)	DT(a.u.)
94	2-Ethyl-5-methylpyrazine	13360-64-0	$C_7H_{10}N_2$	122.2	1000.6	364.099	1.67285
95	2-Heptanone(D)	110-43-0	$C_7H_{14}O$	114.2	886.2	264.439	1.26032
96	Unidentified	*	*	0	783.7	210.374	1.40293
97	Citronellol	106-22-9	$C_{10}H_{20}O$	156.3	1233.4	694.466	1.35178
98	Camphene	79-92-5	$C_{10}H_{16}$	136.2	952.3	319.935	1.62248

CAS: Chemical Abstracts Service registry number; D: dimer; DT: drift time in the drift tube; MW: molecular weight; RI: retention index calculated using n-ketones C_4–C_9 as external standard; RT: retention time in the capillary GC column; The compounds are arranged in increasing order of their RT.

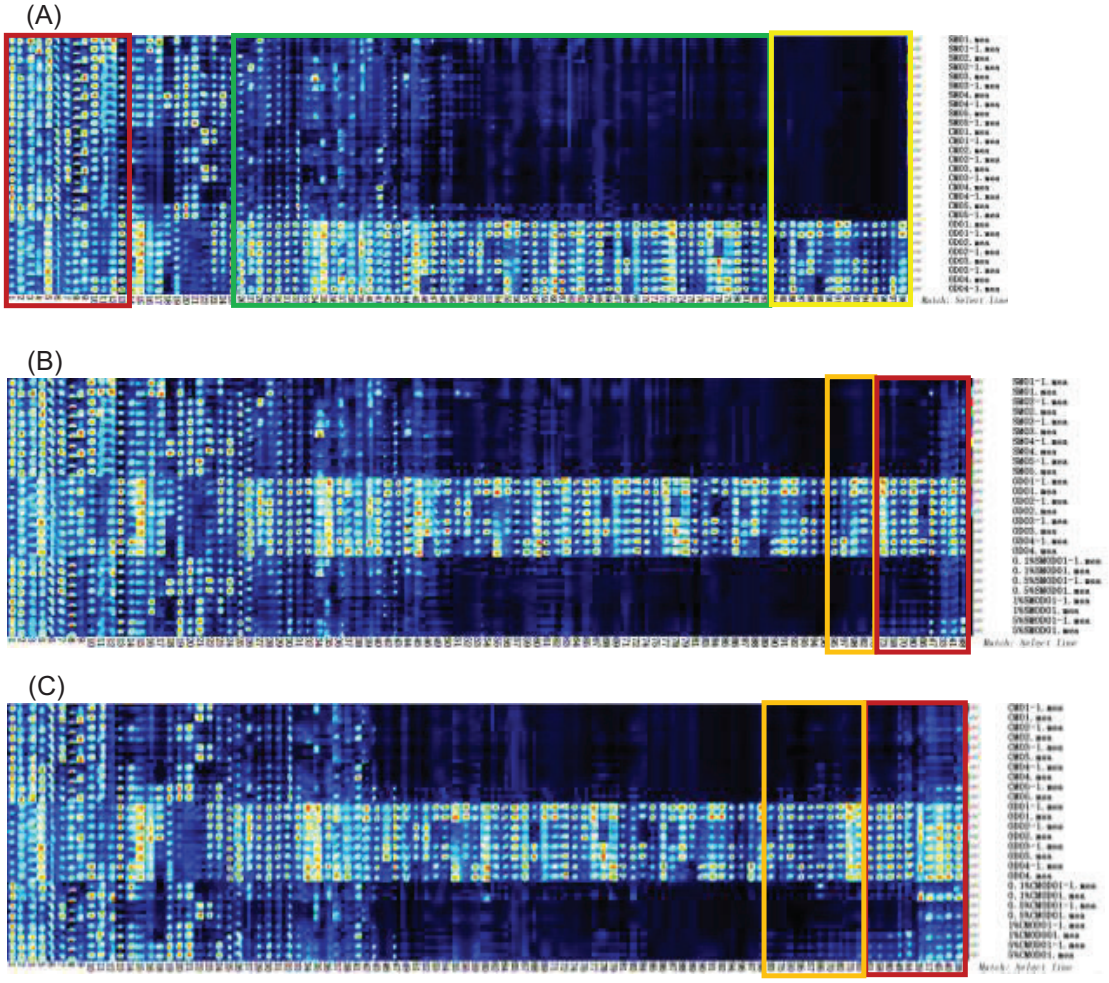

Figure 3. (A) Fingerprints of the volatile components in pure samples, red boxes: Numbers 1–13, green boxes: Numbers 26–83, yellow boxes: 84–98; (B) Fingerprints of the volatile components in SM and adulterated samples; (C) Fingerprints of the volatile components in CM and adulterated samples. Each column represents a volatile compound and each row represents a sample. Numbers correspond to those in Table 1.

discriminate samples with relatively low adulteration ratios (0.1, 0.5, and 1%) from the FPMs. Only adulterants with an OD of 5% could be distinguished from the SM samples based on volatile compounds. Hence, the unsupervised PCA method was inappropriate for discriminating adulterants with OD samples from different FPMs.

The supervised OPLS-DA model used in this study was built to uncover underlying differences. With the 98 VOCs as dependent variables and categories as independent variables, Figure 5(A) shows the clustering of the SM and OD samples obtained using this model. For the evaluation parameters of the model, an R^2X value of

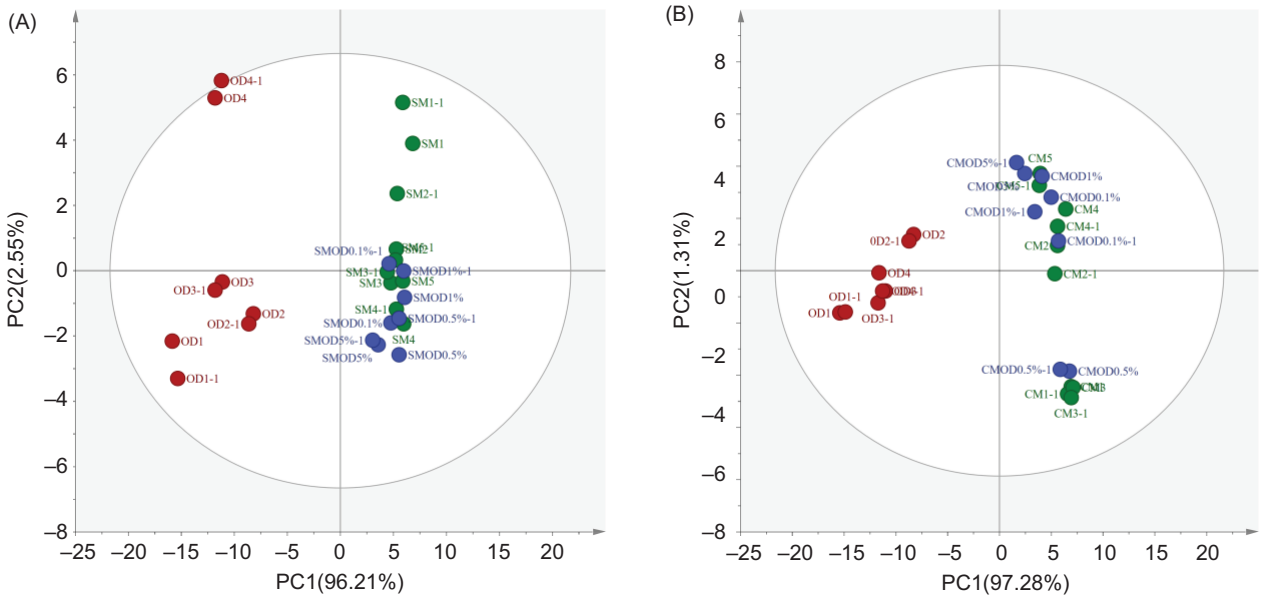

Figure 4. PCA score plot based on the volatile compounds obtained with pure and adulterant samples, (A) SM-OD; (B) CM-OD.

0.733, R^2Y value of 0.781, Q^2 (cum) value of 0.728, and R^2 and Q^2 exceeding 0.5, indicated an acceptable model fit. Notably, the two groups of SM and adulterant samples were well-separated using this model, except for the 0.1% adulterants. The permutation test was performed 200 times. The results of the cross-validation showed that all Q^2 values on the left side were lower than the original point on the right side, and the regression line of Q^2 intersected the vertical axis at a point below 0, as shown in Figure 5(B). This suggests that the models provided a strong fit to the data.

An OPLS-DA model was constructed to represent the adulteration of CM with OD. Figure 5(C) also shows clustering of the DM and OD samples, with an R^2X value of 0.799, an R^2Y value of 0.757, and a Q^2 (cum) value of 0.528. The permutation test was performed 200 times. The results of the cross-validation showed that all Q^2 values on the left side were lower than the original point on the right side, and the regression line of Q^2 intersected the vertical axis at a point below 0, as shown in Figure 5(D). However, CM and adulterants with OD proportions of 0.1 and 0.5% were not separated by this model. For low adulteration levels samples (0.1 and 0.5%), the differential ability of OPLS-DA was limited, mainly due to the low content of the differential VOCs in these samples. However, the results reported for the identification of antibiotic dregs adulteration in feed using attenuated total reflection mid-infrared spectrum are lower compared to ours (Li *et al.*, 2021). Some reports on the illegal use of antibiotic dregs have also shown that the amount of AD adulteration in actual production is always greater than 5%. Hence, the models in this study meet the requirements of market surveillance.

Selection of potential markers

The final purpose of the adulteration detection method is market surveillance. Therefore, the detection results of the methods used for market surveillance should be traceable. Marker-based adulteration detection methods can be traced back to reference standards and are used in arbitration inspections. In this study, the OPLS-DA model was used to extract the variables that greatly contributed to the discrimination between different groups and to explore the critical markers for discrimination. Variables with a VIP > 1 were considered to have the greatest influence on the discrimination method.

In the SM-OD-OPLS-DA model, 46 variables (42 of which were identified) were calculated with a VIP value of > 1, and the average signal intensity difference between SM and OD was calculated, see Figure 6(A). The VIP values of the compounds NO. 48, 57, 58, 60, 61, 63, 64, 67, 69, 70, 71, 72, 73, 74, 77, 79, 80, 81, 82, 91, and 98 were between 1.0 and 1.4. As shown in Figure 3(B), the signal intensities of these compounds in the OD samples were significantly higher than those in the SM samples. In the CM-OD-OPLS-DA model, 53 variables (49 of which were identified) were calculated with a VIP value > 1, and the average signal intensity difference of these compounds between CM and OD was also calculated, see Figure 6(B). Among them, the VIP value of the compounds NO. 39, 47, 48, 49, 50, 57, 58, 60, 61, 63, 64, 67, 69, 70, 71, 73, 74, 77, 80, 82, 87, 91, and 98 were between 1.0 and 1.2. As shown in Figure 3(C), the signal intensities of these compounds in the OD samples were significantly higher than those in the CM samples. Compounds 48, 57, 58, 60, 61, 63, 64, 67, 69, 70, 71, 73, 74, 77, 80, 82, 91, and 98 played

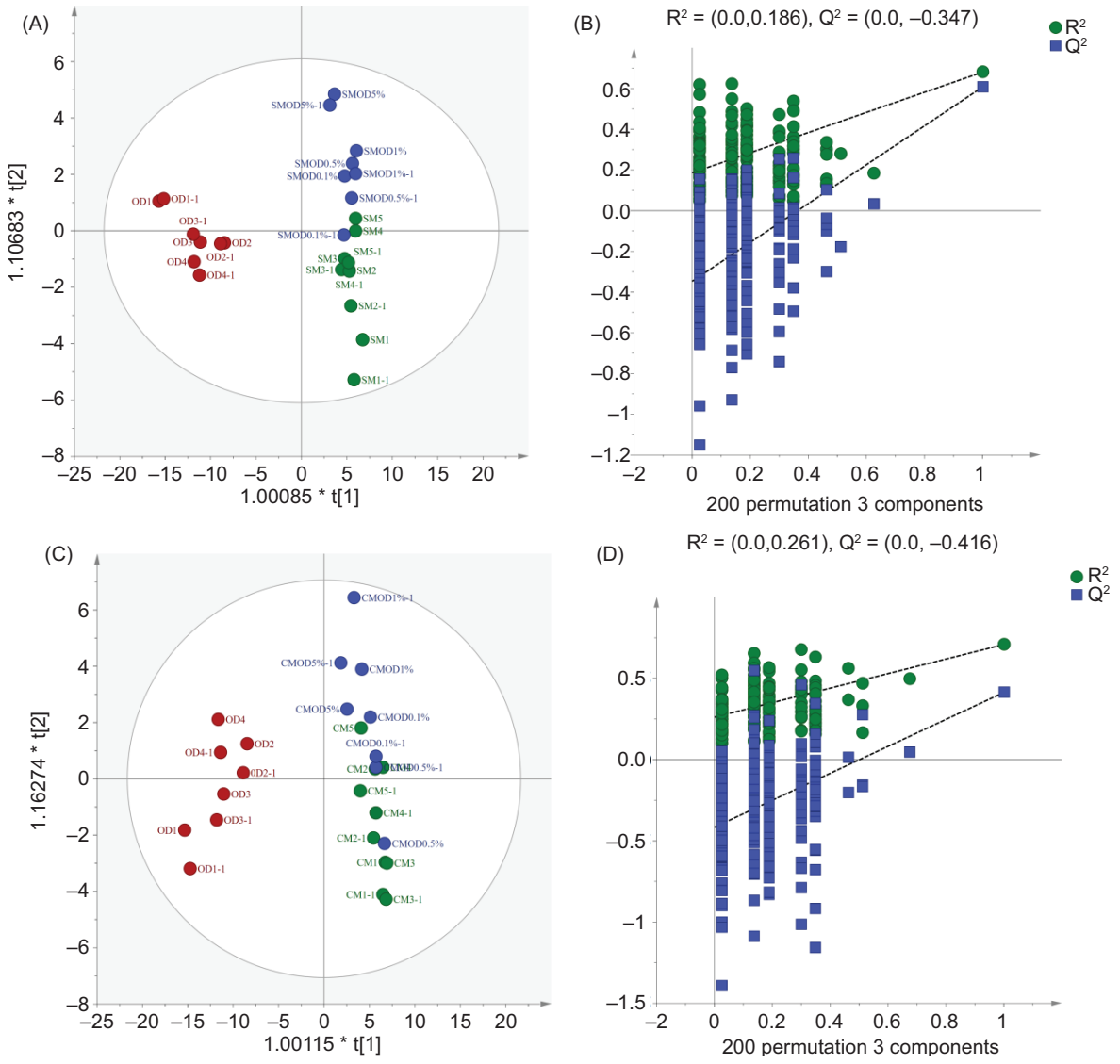

Figure 5. (A) Fingerprints of the volatile components in pure samples; (B) Fingerprints of the volatile components in SM and adulterated samples; (C) Fingerprints of the volatile components in CM and adulterated samples. Numbers correspond to those in Table 1.

important roles in identifying the two OPLS-DA models. Therefore, these 18 compounds (1 ether, 1 heterocycle, 2 acids, 2 terpenes, 3 ketones, 3 alcohols, 3 aldehydes, and 3 esters) were selected as potential markers for detecting FPMs adulteration with OD.

Conclusions

HS-GC-IMS was used to detect the adulteration of SM and CM samples with OD. A total of 98 VOCs were detected in 14 pure samples. The individual compounds belonged to eight categories: esters, aldehydes, alcohols, ketones, acids, heterocycles, ethers, and terpenes. PCA and OPLS-DA indicated the ability of HS-GC-IMS to discriminate between the pure SM, CM, and OD samples based on their volatile profiles. The OPLS-DA model distinguished SM and CM from the adulterants when the adulteration ratios were as low as 0.5 and 1%, respectively. Eighteen volatile substances (1 ether, 1 heterocycle, 2 acids, 2 terpenes, 3 ketones, 3 alcohols, 3 aldehydes, and 3 esters) were proposed as key markers for OD authentication in SM and CM samples. The analysis demonstrated that HS-GC-IMS combined with a chemometric method provides a rapid, accurate, and simple approach for detecting the adulteration of feed protein materials. Because of its relatively low cost, HS-GC-IMS can be used as a powerful authentication tool to control the quality of feed protein materials.

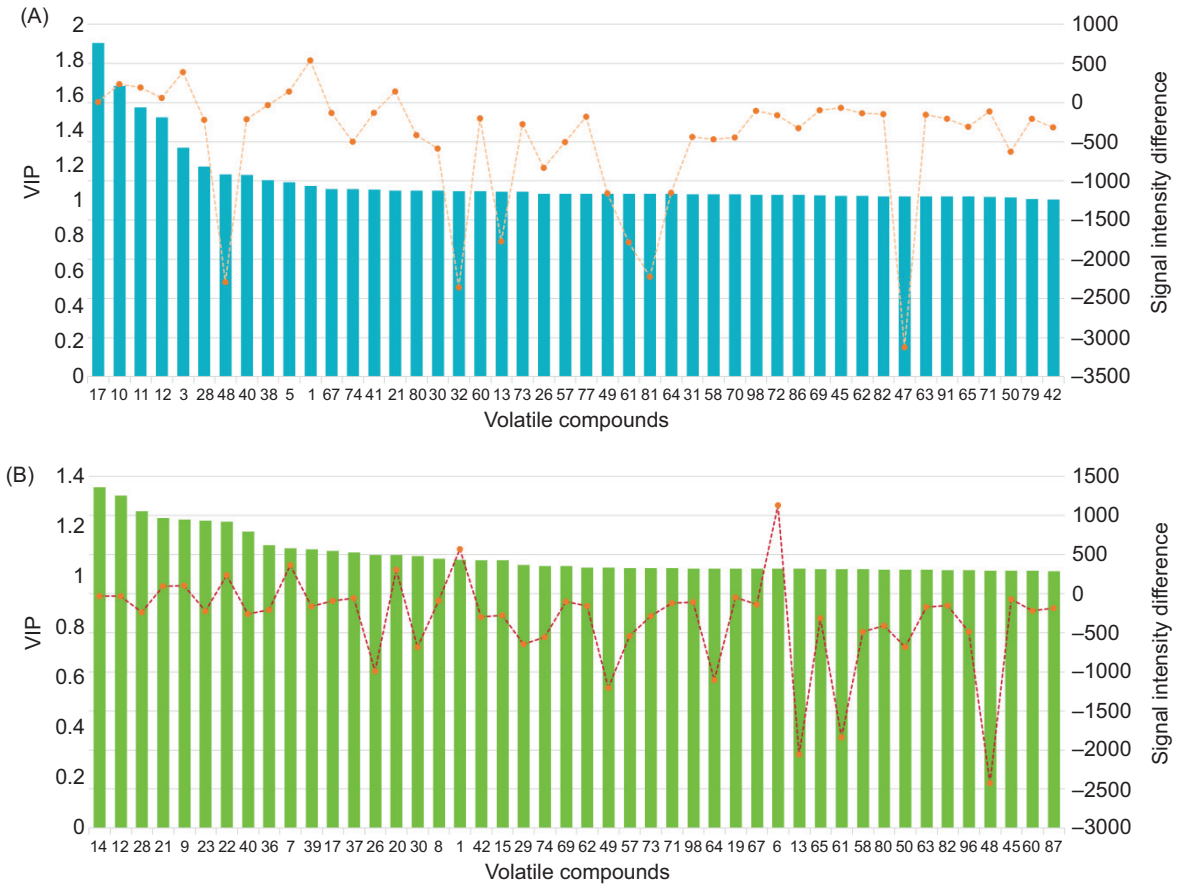

Figure 6. The VIP and signal intensity difference values of potential biomarkers of OPLS-DA models. (A) SM-OD and (B) CM-OD.

Nevertheless, factors such as sample type, size, and representatives may influence the generalizability and applicability of the HS-GC-IMS method. Moreover, the volatile organic compounds in the sample may change under different environmental or storage conditions. Thus, future studies should investigate these environmental factors and sample differences (including increasing sample types and extending sample storage time) to improve the robustness and reliability of HS-GC-IMS.

Authors Contributions

Shouxue Li: Writing the original draft, methodology, investigation; Yuchao Feng, Yushu Zhang: Visualization, data curation, software; Xia Fan: Writing the review & editing, project administration, funding acquisition.

Conflicts of Interest

The authors declare no conflict of interest.

Funding

This work was financially supported by the Science and Technology projects plan of Jiangsu Vocational College of Agriculture and Forestry (Grant No. 2022kj17 and 2022kj04), Xinjiang "Two Regions" Science and Technology Development Program of China (2023LQ02002).

References

Arroyo-Manzanares, N., García-Nicolás, M., Castell, A., Campillo, N., Viñas, P., López-García, I. and Hernández-Córdoba, M., 2019. Untargeted headspace gas chromatography—Ion mobility spectrometryanalysis for detection of adulterated honey. Talanta 205: 120123. https://doi.org/10.1016/j.talanta.2019.120123

Dou, X., Zhang, L., Yang, R., Wang, X., Yu, L., Yue, X., et al., 2022. Adulteration detection of essence in sesame oil based on headspace gas chromatography-ion mobility spectrometry. Food Chemistry 370: 131373. https://doi.org/10.1016/j.foodchem.2021.131373

Gu, S., Zhang, J., Wang, J., Wang, X. and Du, D., 2021. Recent development of HS-GC-IMS technology in rapid and nondestructive detection of quality and contamination in agri-food products. Trends in Analytical Chemistry 144: 116435. https://doi.org/10.1016/j.trac.2021.116435

Guo, B., Gong, L., Duan, E., Liu, R., Ren, A., Han, J., et al., 2012. Characteristics of penicillin bacterial residue. Journal of the Air & Waste Management Association 62(4): 485–488. https://doi.org/10.1080/10962247.2012.658956

Harris, E.K., Mellencamp, M.A., Johnston, L.J., Cox, R.B. and Shurson, G.C., 2018. Effectiveness of different corn dried distiller grains with solubles feeding strategies and increasing the time intervals between the second Improvest dose and slaughter of immunologically castrated pigs on belly and pork fat quality. Meat Science 135: 62–73. https://doi.org/10.1016/j.meatsci.2017.08.025

Hernández-Mesa, M., Ropartz, D., García-Campaña, A.M., Rogniaux, H., Dervilly-Pinel, G. and Le Bizec, B., 2019. Ion mobility spectrometry in food analysis: Principles, current applications and future trends. Molecules 24(15): 2706. https://doi.org/10.3390/molecules24152706

Kim, S.W., Less, J.F., Wang, L., Yan, T.H., Kiron, V., Kaushik, S.J., et al., 2019. Meeting global feed protein demand: Challenge, opportunity, and strategy. Annual Review of Animal Biosciences 7: 221–243. https://doi.org/10.1146/annurev-animal-030117-014838

Kranenburg, R.F., Verduin, J., Stuyver, L.I., de Ridder, R., van Beek, A., Colmsee, E., et al., 2020. Benefits of derivatization in GC-MS-based identification of new psychoactive substances. Forensic Chemistry 20: 100273. https://doi.org/10.1016/j.forc.2020.100273

Li, C., Zhang, G., Zhang, Z., Ma, D. and Xu, G., 2016. Alkaline thermal pretreatment at mild temperatures for biogas production from anaerobic digestion of antibiotic mycelial residue. Bioresource Technology 208:49–57. https://doi.org/10.1016/j.biortech.2016.02.064

Li, S.X., Fan, X., Wu, Y.L., Liao, K.K., Huang, Y.P., Han, L.J., et al., 2021. A novel analytical strategy for discriminating antibiotic mycelial residue adulteration in feed based on ATR-IR and microscopic infrared imaging. Spectrochimica Acta Part A: Molecular and Biomolecular Spectroscopy 261: 120060. https://doi.org/10.1016/j.saa.2021.120060

Lin, Y., Yang, Z., Liang, H., Li, S., Fan, X. and Xiao, Z., 2018. Identification of antibiotic mycelia residue in protein rich feed using on near-infrared microscopy imaging. Food Additives & Contaminants 35(5): 818–827. https://doi.org/10.1080/19440049.2018.1429675

Mohring, S.A.I., Strzysch, I., Fernandes, M.R., Kiffmeyer, T.K., Tuerk, J. and Hamscher, G., 2009. Degradation and elimination of various sulfonamides during anaerobic fermentation: A promising step on the way to sustainable pharmacy? Environmental Science & Technology 43(7): 2569–2574. https://doi.org/10.1021/es802042d

Mottet, A., de Haan, C., Falcucci, A., Tempio, G., Opio, C. and Gerber, P., 2017. Livestock: On our plates or eating at our table? A new analysis of the feed/food debate. Global Food Security 14: 1–8. https://doi.org/10.1016/j.gfs.2017.01.001

Rodríguez, S.D., Rolandelli, G. and Buera, M.P., 2019. Detection of quinoa flour adulteration by means of FT-MIR spectroscopy combined with chemometric methods. Food Chemistry 274: 392–401. https://doi.org/10.1016/j.foodchem.2018.08.140

Song, X.C., Canellas, E., Asensio, E. and Nerin, C., 2020. Predicting the antioxidant capacity and total phenolic content of bearberry leaves by data fusion of UV-Vis spectroscopy and UHPLC/Q-TOF-MS. Talanta 213: 120831. https://doi.org/10.1016/j.talanta.2020.120831

Tian, H., Xiong, J., Chen, S., Yu, H., Chen, C., Huang, J., et al., 2023. Rapid identification of adulteration in raw bovine milk with soymilk by electronic nose and headspace-gas chromatography ion-mobility spectrometry. Food Chemistry: X 18: 100696. https://doi.org/10.1016/j.fochx.2023.100696

Wang, S., Chen, H. and Sun, B., 2020. Recent progress in food flavor analysis using gas chromatography-ion mobility spectrometry (GC-IMS). Food Chemistry 315: 126158. https://doi.org/10.1016/j.foodchem.2019.126158

Yan, H., Li, P., Zhou, G., Wang, Y., Bao, B., Wu Q., et al., 2021. Rapid and practical qualitative and quantitative evaluation of non-fumigated ginger and sulfur-fumigated ginger via Fourier-transform infrared spectroscopy and chemometric methods. Food Chemistry 341(Pt 1): 128241. https://doi.org/10.1016/j.foodchem.2020.128241

Yang, X., Xing, B., Guo, Y., Wang, S., Guo, H., Qin, P., et al., 2022. Rapid, accurate and simply-operated determination of laboratory-made adulteration of quinoa flour with rice flour and wheat flour by headspace gas chromatography-ion mobility spectrometry. LWT–Food Science and Technology 167: 113814. https://doi.org/10.1016/j.lwt.2022.113814

Yang, X., Zhu, K., Guo, H., Geng, Y., Lv, W., Wang, S., et al., 2021. Characterization of volatile compounds in differently coloured *Chenopodium quinoa* seeds before and after cooking by headspace-gas chromatography-ion mobility spectrometry. Food Chemistry 348: 129086. https://doi.org/10.1016/j.foodchem.2021.129086

Zhang, X., Dai, Z., Fan, X., Liu, M., Ma, J., Shang, W., et al., 2020. A study on volatile metabolites screening by HS-SPME-GC-MS and HS-GC-IMS for discrimination and characterization of white and yellowed rice. Cereal Chemistry 97(2): 496–504. https://doi.org/10.1002/cche.10264